

## A NEW PROCEDURE FOR AIRFOIL DEFINITION

P. VENKATARAMAN\*  
Rochester Institute of Technology  
Rochester, New York

### Abstract

A new technique for single element airfoil definition is advanced in this paper. The airfoil geometry is obtained through four Bezier polygons, two for the top surface, and two for the bottom surface. Unlike traditional procedures, the method identifies the airfoil shape without the superposition of camber distribution, thickness distribution, nose radius, trailing edge angle or ideal aerodynamic coefficients. The method is compared against airfoils that represent both traditional shapes as well as contemporary ones. The Bezier emulation is also documented with respect to the ideal solution using a basic panel method. It is shown that the new procedure is an acceptable alternative to conventional airfoil definition. There are significant advantages for the geometry created with this new procedure, namely, accommodation of structural constraints and/or constraints due to manufacture; easy use of CFD software that can accept spline based geometry; and use of optimization techniques to design for specific performance. The method also easily accommodates special airfoil shapes like a droop nose or a blunt trailing edge.

### 1. Introduction

Synthesis of new airfoil shapes continues to remain an important area of aerodynamic design. With the increasing use of Computational Fluid Dynamics (CFD) in the design of airfoils as well as the flight vehicle itself, there is little adherence to traditional procedures for describing the airfoil geometry, since the analysis is driven by the overall surface coordinates rather than the details of the construction of the shape. The traditional identification of the airfoil geometry generally includes the superposition of camber and

thickness distributions, along with a blending nose radius, a trailing edge description, and maybe the value of the ideal lift coefficient.

A new method of generating the airfoil geometry using Bezier parameterization was introduced last year at the Applied Aerodynamics Conference<sup>[1]</sup>. In the same meeting, Reference 2, also used a similar approach for establishing the symmetrical airfoil geometry. In this paper the method is extended to traditional and contemporary airfoils. Airfoils with special shapes are easily obtained by the creative use of the construction procedure. It is hoped there is sufficient evidence presented in this paper to redefine the way airfoil geometry is generated in the future.

Four airfoils are chosen for this presentation. Between them they include the useful, the conventional, the contemporary, and a non-traditional one that suggests the universality of the construction technique. The first is from the NACA six digit series NACA 653-418<sup>[3]</sup>. The second is the Wortmann FX63-167<sup>[4]</sup>. The third is due to Selig S1223<sup>[5]</sup>, a low Reynolds number airfoil, presented at the last years meeting. The final one is the classical Liebeck optimal airfoil, identified here as L1969<sup>[6]</sup>.

The method of construction is kept the same for all the airfoils, even though the technique is very flexible to adapt easily to the geometry that is being simulated. All the Bezier emulations are shown in enlarged ordinate scale to indicate the goodness of fit.

The actual construction involves generating four Bezier parametric curves for each airfoil. There are two curves for the top and two for the bottom surface. The curves on adjacent surfaces share a common vertex. The Bezier curves are determined completely by identifying the vertices of the respective polygons used to generate the parametric curve. The parametric curves are cubic in each polygon.

---

\*Assistant Professor, Dept. of Mechanical Engineering  
Rochester Institute of Technology, Senior Member AIAA

The Bezier polygons are obtained by formulating a constrained least-squared error problem between the original airfoil coordinates and those obtained using the Bezier polygons. This is solved using a technique from traditional design optimization, namely the Generalized Reduced Gradient Method (GRG)<sup>[7]</sup>.

An important concern with the new technique of identifying the airfoil geometry is the preservation of the aerodynamic characteristics of the original geometry. A basic panel method<sup>[8]</sup> (ideal solution) was used for comparison with respect to the original and the fitted geometry. Only a single point comparison is made.

In the following work, it is shown that the proposed technique provides an effective procedure for the description of airfoil geometry.

## 2. Bezier Parameterization

Bezier parametric curves are usually recommended for *ab initio* designs. Such designs are characterized by both aesthetic and functional requirements. These curves are special cases of uniform B-splines. Today non-uniform rational B-splines (NURBS) are important elements for defining surfaces and shapes in computer aided design (CAD), finite element analysis (FEM) and CFD, and even complete aerospace vehicles. The extension of the two-dimensional ideas presented here to define wings and aerodynamic surfaces should be possible without any difficulty.

The Bezier parameterization is based on the Bernstein basis functions. There are several features of the Bezier description that make it very useful for the definition of the airfoil geometry<sup>[9]</sup>. Figures 1a and 1b are examples of cubic Bezier curves used in the airfoil construction. The following are some useful properties of Bezier curves:

- (i) The basis functions are real.
- (ii) The degree of polynomial defining the curve is one less than the number of polygon vertices. In this paper, the number of vertices for each curve is maintained at four for all the airfoils. This generates a cubic Bezier curve in each segment. The only consideration for this choice was the traditional practice of 'lofting' used for engineering drawings of the airfoil shapes. The choice can be controlled by the designer of the shape, without any significant increase in the effort required to generate it.

Conventional NACA four and five digit thickness sections include inverse square root and quartic dependencies.

- (iii) The first and the last points of the curve are coincident with the first and last points of the defining polygons.
- (iv) The slope at the ends of the curve have the same direction as the polygon sides.
- (v) The curve is contained within the convex hull of the defining polygon.
- (vi) The curve is invariant under an affine transformation.

The cubic Bezier curve in this discussion is generated by a polygon with four vertices;  $B_0$ ,  $B_1$ ,  $B_2$ , and  $B_3$ . Each  $B_i$  corresponds to a pair of values in two-dimensional space. Any point  $P(x,y)$  on the Bezier curve corresponds to a parameter  $\nu$ , which ranges between 0 and 1 ( $0 \leq \nu \leq 1$ ).  $P(x,y)$  is obtained as

$$P(\nu) = \begin{bmatrix} x \\ y \end{bmatrix} = \sum_{i=0}^3 B_i J_{3,i}(\nu) \quad (1)$$

The Bernstein basis  $J_{3,i}$  is given as :

$$J_{3,i}(\nu) = \begin{bmatrix} 3 \\ i \end{bmatrix} \nu^i (1 - \nu)^{3-i} \quad (2)$$

where the coefficient on the right represents the combination  ${}^3C_i$ .

## 3. Airfoil Construction

A typical airfoil is constructed using four such Bezier polygons each of them referred as a segment. Two of them determine the top surface and two the bottom [see Figures 2 and 3].

The forward segments on the top and the bottom surface share the leading edge. The leading edge can be accurately identified by requiring the three adjoining vertices, with the leading edge in the middle, to lie on a vertical line. The trailing edge point is shared by the rear segments of the top and the bottom surface. Blunt trailing edges can be designed by providing each rear surface with its own trailing edge point.

Each pair on the same surface share a common vertex. For slope continuity, it is essential that the three adjoining vertices, with the shared vertex in the middle, lie on a straight line. Figure 2, illustrates an example of the upper surface of the basic NACA

symmetric thickness distribution. Here the three vertices lie on a line parallel to the x-axis. This special geometry is enforced for all the airfoils studied in this paper as it clearly identifies the location of the maximum thickness of the top section. All airfoils appear to subscribe to this geometry for the upper surface. Similar description is used for the bottom surface in this paper. For contemporary airfoils, because of the inflection of the lower surface, this particular imposition may have less utility for the geometry description, but will accommodate manufacturing or structural constraints.

Figure 3 illustrates the four segments, s1 through s4, used for the construction of a general airfoil. Each segment is identified through four vertices. The four vertices then allow us to construct a cubic parametric curve in the segment. In this study, the parameter values are chosen at equal intervals. For a general airfoil the abscissa values will be at non uniform intervals. It is possible to choose varied intervals for the parameter values so that more points are clustered at the leading edge to enable a better solution to the subsequent aerodynamic analysis. This is not used in this presentation.

In the following, the effectiveness of this new procedure is illustrated by recreating existing airfoils using the above technique. Four airfoils are chosen for study. Three of the airfoils represent traditional and contemporary airfoils. They are NACA 653-418, Wortmann FX63-167, and Selig S1223. The fourth, due to Liebeck, L1969 is quite different from conventional geometry and was chosen to challenge the technique. While four airfoils is a small sample, there was absolutely no difficulty in applying the ideas being advanced in this paper. The author is quite confident that the procedure can be universally applied.

#### 4. Airfoil Emulation

New airfoils and their coordinates can be created by defining the polygon vertices from which the shape can be obtained. For existing airfoils, the coordinates are available. The problem is therefore to identify the polygon vertices which will reproduce the original airfoils, using the Bernstein basis identified in Eqs. 1-2.

This problem of determining the unknown polygon vertices is set up as an unorthodox non-linear least-squared error problem, where the error is the difference between the original coordinates and the fitted Bezier curves obtained using the polygon vertices. Constraints are introduced to enforce the geometry of

the polygon, especially the order of abscissa values and the relative locations of the ordinates. These constraints are linear.

The linear constraints and the cubic parametric curve can be easily handled by methods of design optimization. These methods are well documented and many software packages are available that can address this problem. In this paper the solution was obtained using the GRG method applied through an Unix based window driven software called OptdesX<sup>[10]</sup>. The method is not discussed here. The application of the method requires the formulation of the problem of determining the polygon vertices in the format of a standard optimization problem. This requires the identification of design variables, the objective function and constraints. The method is a gradient based technique, where the gradients are obtained numerically. Only local optimum is obtained.

The design variables are some of the vertices of the Bezier polygon. The following specific geometry of the polygons was adopted in this work. The leading edge and trailing edge is assumed to be prescribed. The shared vertex on both the upper and the lower surface identifies the maximum ordinate location. The leading edge is accurately located. Referring to Figure 3, this requires the complete determination of vertices B13, B23, B32, B33; the abscissa values for B14, B22, B34, B42 ; and the ordinate values B12, B43. This provides a total of 14 unknowns which will be the design variables of the problem. It is important to recognize that the fit obtained is the best for this specific geometry. If all the vertices (except for the leading edge and trailing edge) are considered as unknowns then there would be 20 design variables. In optimization problems there is always a need to keep the dimensionality of the problem as low as possible. The software used in this work does not make it any more difficult with the increased number of design variables. The problem however can be anticipated if this search for the airfoil shape is coupled with aerodynamic analysis. There will be tremendous pressure to keep the number of unknowns to a minimum, and still provide a decent emulation of the shape. Following standard practice the chord is normalized to 1 for all the airfoils emulated.

The objective is to minimize the sum of the squares of the error between the original ordinates and the Bezier fitted ordinates obtained from the polygon vertices. The constraints are the order of the abscissa values of the vertices of the polygon, as well as the relation between adjacent ordinates to enforce a typical

airfoil shape. These are developed as linear constraints between some of the adjacent design variables. There are about 22 of them for the problem formulated here. It is also necessary to place range constraints on each design variable to limit the design space to a reasonable volume. Care should be taken that this range does not restrict the search for the best solution.

### 5. Bezier Simulation of Existing Airfoils

The four airfoils mentioned earlier are fitted with cubic Bezier parametric curves. For each airfoil a comparison is also made of the ideal normalized velocity using the Hess-Smith-Douglas panel method<sup>[8]</sup>. The panels are made of adjacent coordinates, the number and location being dictated by the original data. A single point comparison was made at an angle of attack of 4 degrees. For the ideal flow, the Reynolds number has no significance. The Bezier polygons are not shown as they are only incidental to the determination of the airfoil shape.

All calculations were performed on the Digital Equipment Corporation workstation 5000 using double precision arithmetic. The initial shape for all the airfoils was an arbitrary symmetrical section. The final solution was achieved in about 20 iterations. Gradients were computed numerically using forward difference with a perturbation of  $\epsilon = 0.0001$ .

**(i) NACA 653-418** Figure 4 is a comparison of the original airfoil and the shape simulated using Bezier parametric curves. The ordinate scale is enlarged to demonstrate the nature and accuracy of fit. Except for the region around the nose in the top forward segment, the fit is very good. The overall squared error over 50 data points was  $3.0 \times 10^{-5}$ .

Figure 5 is a comparison of the ideal velocity distribution. The number of panels was 49. Once again except for three data points at the leading edge on the top surface, the curves agree to a remarkable degree. The counter clockwise definition of the panels from the trailing edge makes the velocity on the bottom negative. The lift coefficient ( $C_l$ ) for the original data was 0.768.  $C_l$  for the Bezier geometry was 0.789. The published value is 0.76. This is an error of 2.7 % for the Bezier geometry compared to the original geometry.

**(ii) Wortmann FX63-167** Figure 6 is the comparison of the original geometry and that obtained using Bezier curves. The reproduction through the parametric

curves is very good. Note that there is a point of inflection for the lower surface. In spite of the particular geometry imposed ( a single minimum is expected for the lower surface), the technique does not appear to have any problems in achieving the remarkable fit. The overall squared error over 96 data points was  $2.0 \times 10^{-5}$ .

Figure 7 is the comparison of the ideal velocity distribution between the original and the Bezier geometry. The number of panels was 95. Very small differences are observed near the leading edge on the upper surface, and at the trailing edge. The  $C_l$  for the original airfoil calculated by the program was 1.541. The  $C_l$  due to the Bezier geometry was 1.494. This is an error of 3.05 %.

**(iii) Selig S1223** Figure 8 is the comparison of the original airfoil and the geometry simulated using the Bezier curves. There appears a slight increase in maximum thickness of the top surface, which coincides with the increase in  $C_l$ . Once again, there is a point of inflection on the bottom surface while the fitted geometry is expected to have a single minimum. Refitting the original airfoil by imposing a geometry that locates a point of inflection is just as easy as the current exercise. This would require the vertices B42, B34, and B33 to remain on a line inclined to the  $x/c$  axes. It was decided to continue with the current fit for consistency and to expose any problems with the technique. Nevertheless the fit is good except for the region around  $x/c = 0.1$ . The flattening of the airfoil at this point is due to the imposed geometry that locates the vertex B34(B41) around this point. The abscissa values for the B42, B34, B33 vertices are .04323, 0.12667, and 0.12070 respectively. The  $x/c$  location of the vertex B33 and B34 differ only by 0.00037. The overall squared error over 80 data points was  $3.0 \times 10^{-5}$ .

Figure 9 is the comparison of the ideal velocity distribution for the Selig airfoil. Except for the trailing edge, the fit is quite reasonable. The extension of the lower pressure on the top and the slightly lower velocity on the bottom provide an increase in the lift coefficient. The flattening of the airfoil, introduces a slight kink on the velocity distribution. The number of panels was 79. The  $C_l$  for the original shape was 1.824. The  $C_l$  for the Bezier shape was 2.006 giving an error of 4.26 %.

**(iv) Liebeck L1969** Figure 10 is the comparison between the original airfoil and the Bezier simulation.

Unlike the remaining airfoils, the information on the location of the leading edge was not available. The leading edge of all the previous airfoils was at (0.0,0.0). In this case the leading edge was assumed to be at (0.0,0.28) from inspection. The assumed geometry requires the specification of the leading edge. The original profile appears to be flatter on the top surface, while the bottom surface is approximated well by the Bezier curve.

Figure 11 is the comparison of the ideal velocity distribution for this airfoil. There is some discrepancy in the region of minimum pressure. The number of data points were 96. The number of panels was 95. The  $C_l$  due to the original shape was 3.603 while that due to the fitted geometry was 3.615 giving an error of 0.3 %. This low error is deceiving in the light of the Figure 11. With a better estimate for the location of the leading edge it may be possible to reduce this error.

It should be noted that the fitted curves are all cubic, irrespective of the variation involved in the original geometry. All the curves have been obtained in exactly the same manner without exploiting any special features of the original shape. With this technique the airfoil designer has flexibility to explore shapes that conform to other geometries. He can also increase the order of the Bezier curves which will provide additional vertices for control.

#### 6. Special Airfoil Shapes

Special airfoil geometry can be obtained by the creative use of the construction procedure. This can be obtained primarily by selecting a similar feature in the respective polygon that generates the curve. The polygon will reflect to some extent the nature of the overall shape. Figure 3 is referenced for the following discussion.

(i) Nose Droop Figure 12 indicates an example of nose droop. One way to achieve this is to move the vertex B42 out of the straight line alignment with B34 and B33. Here the vertex has just been moved down at the same x location.

(ii) Blunt Trailing Edge Figure 13 is an example of a blunt trailing edge. This was achieved by providing the rear segments to have their own vertex instead of sharing one as was done in the previous study. Here the ordinate of B24 was moved up.

(iii) Cusped Trailing Edge A cusp at the trailing edge

can be obtained by controlling the alignment of B23 and B24, and B31 and B32 for the top and bottom surfaces respectively. The figure is not shown.

Many other geometric features can be obtained by adjusting the vertices of the polygon.

(iv) Structural Constraints Structural or manufacturing constraint can easily be built into the geometry definition. The maximum thickness location for the top surface can be controlled by requiring the vertices B13, B14 and B22 to lie on a horizontal line. The vertex B14 locates the maximum thickness.

Similar design can be incorporated for the bottom surface by controlling the vertices B42, B34 and B33. The maximum thickness of the top and the bottom can be designed to have the same value of the abscissa which would be of tremendous help in structural design and manufacture. For wing design, it is possible to vary the airfoil shape along the span while maintaining the same location for the maximum thickness so that straight spars can be designed. This will be most advantageous for the design of the helicopter blades.

(v) Leading Edge Definition The geometry used for defining the leading edge on the top surface appears to be adequate in this presentation. Higher order Bezier curves can be used to control the surface definition for improvement in the velocity gradients and boundary layer growth. This would provide additional vertices that can be chosen by the designer. The construction procedure itself does not change. Higher order curves can be easily incorporated into the procedure.

#### 7. Conclusions

A new technique for single element airfoil definition is presented in this paper. The construction involves determining four cubic parametric curves, two for the top surface and two for the bottom surface. The curves can be automatically generated by identifying the vertices of the polygons that contain them while respecting the geometric constraints the vertices need to satisfy. There is no need for thickness distribution, camber distribution, nose radius or any other information to generate the airfoil. Four existing airfoils are recreated using the procedure. The method is shown to emulate the original airfoils fairly well. Comparison of ideal flow aerodynamics using a basic panel method show a reasonable agreement between the original and the emulated geometry. In some of the

cases, the quality of emulation could have been increased by incorporating geometric features of the original airfoil for the location of the vertices. This exercise was to validate the method using a consistent approach. The results indicate that the new procedure discussed in the paper is an effective way to determine airfoil shapes. Extensions to wings should be possible without difficulty.

The method naturally allows generation of special shapes by the creative use of the procedure. There are several significant advantages for the geometry created with this procedure, namely the ability to incorporate structural constraints, manufacturing constraints, integration with software that accept spline based definition, and the use of optimization techniques to tailor airfoils for specific performance<sup>[11]</sup>.

### 8. References

1. Venkataraman, P., *A Design Optimization Techniques for Airfoil Shapes*, Paper AIAA 94-1813, 12<sup>th</sup> AIAA Applied Aerodynamics Conference, Colorado Springs, CO, June 1994.
2. Huddleston, D.H., Soni, B.K., and Zheng, X., *Application of a Factored-Relaxation Scheme to Calculation of Discrete Aerodynamic Sensitivity Derivatives*, Paper AIAA-94-1894, 12<sup>th</sup> AIAA Applied Aerodynamics Conference, Colorado Springs, CO, June 1994.
3. Abbot, I.H., and Von Doenhoff, A.E., *Theory of Wing Sections*, Dover Publications, 1959.
4. Althaus, D., and Wortmann, F.X., *Stuttgarter Profilkatalog, Experimental Results from Laminar Wind Tunnel of the Institut für Aero- und Gasdynamik der Universität Stuttgart*, Friedr. Vieweg and Sohn, Braunschweig/Weiebaden.
5. Selig, M., and Guglielmo J.J., *High-Lift Low Reynolds Number Airfoil Design*, Paper AIAA 94-1866, 12<sup>th</sup> AIAA Applied Aerodynamics Conference, Colorado Springs, CO, June 1994.
6. Liebeck, R.H., and Allen, I.O., *Optimization of Airfoils for Maximum Lift*, Journal of Aircraft, Vol. 7, No. 5, 1969.
7. Vanderplaats, G.N., *Numerical Optimization Techniques for Engineering Design, with Applications*, McGraw-Hill Series in Mechanical Engineering, 1984.
8. Moran, J., *An Introduction to Theoretical and Computational Aerodynamics*, John Wiley and Sons, 1984.
9. Rogers, D.F., and Adams, J.A., *Mathematical Elements for Computer Graphics*, McGraw-Hill Publishing Company, 1990.
10. Parkinson, A., et. al., *OptdesX - A Software System for Optimal Engineering Design*, Design Synthesis Inc., Provo, Utah, 1992.
11. Venkataraman, P., *Optimum Airfoil Design in Viscous Flows*, Paper 95-1876, AIAA 13<sup>th</sup> Applied Aerodynamics Conference, San Diego, Ca, 1995.

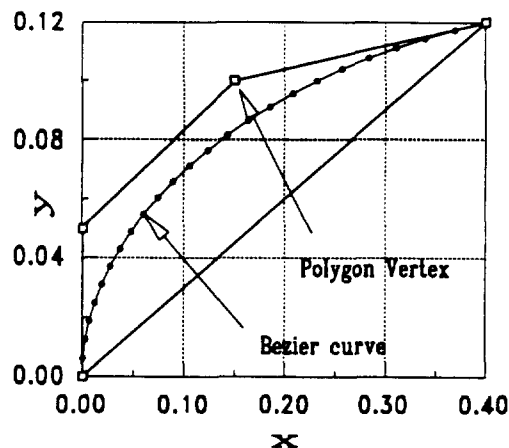


Figure 1a. Example of a Cubic Bezier Curve

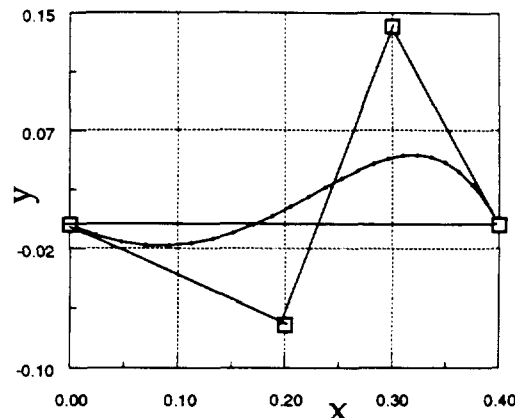


Figure 1b. Example of a Cubic Bezier Curve

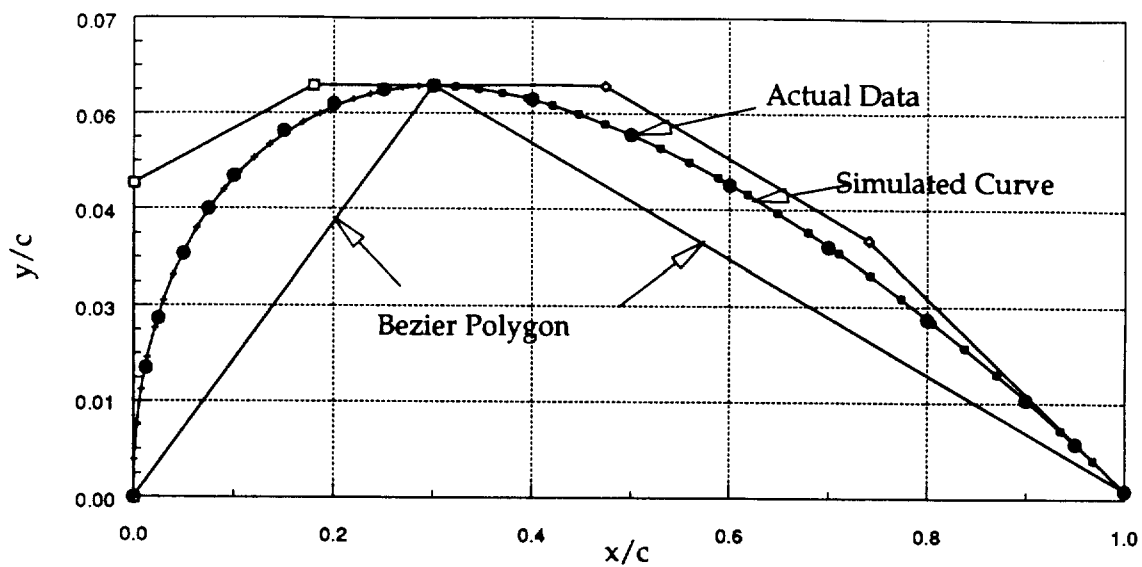


Figure 2. Bezier Emulation of Upper Surface

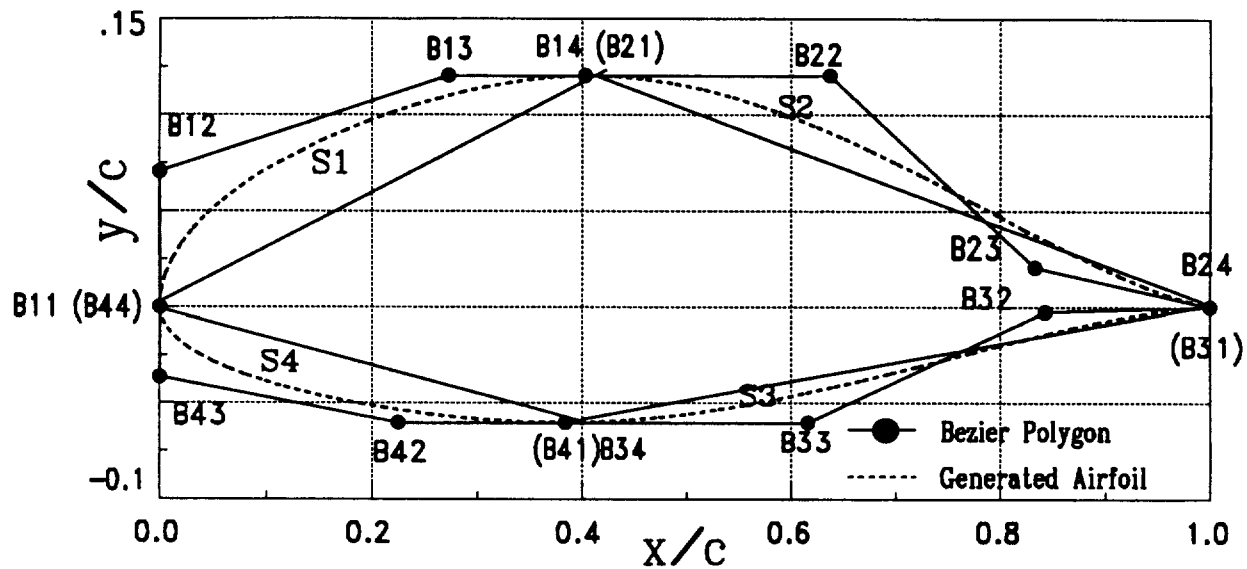


Figure 3. Segments and Polygon Vertices for Airfoil Geometry

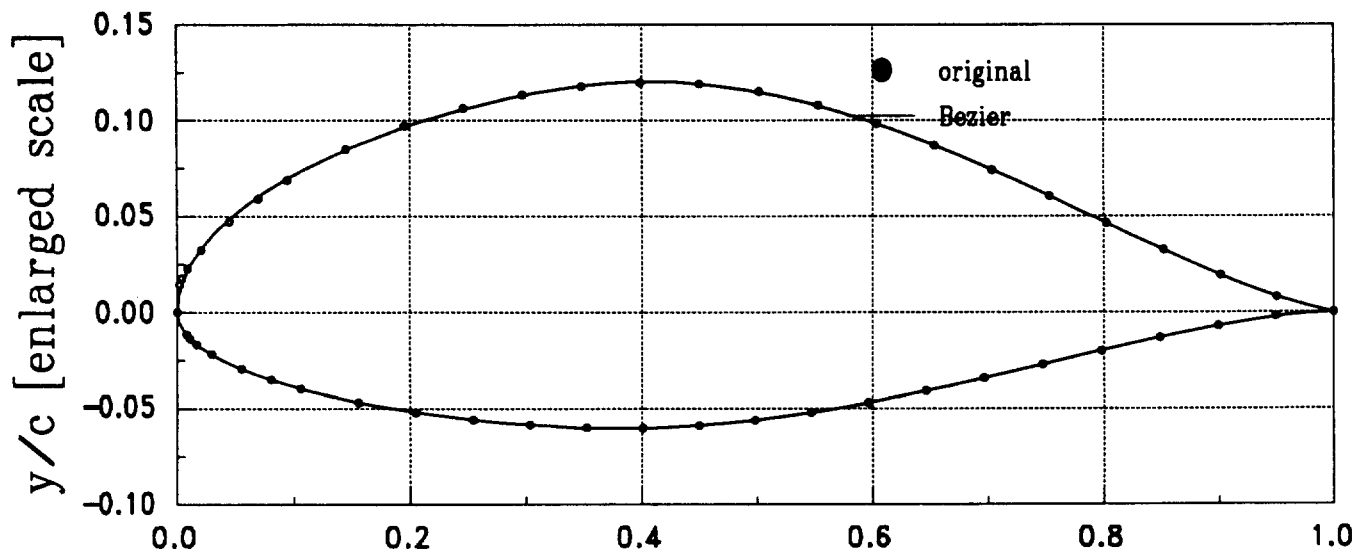


Figure 4. NACA 653-418 - Original and Bezier

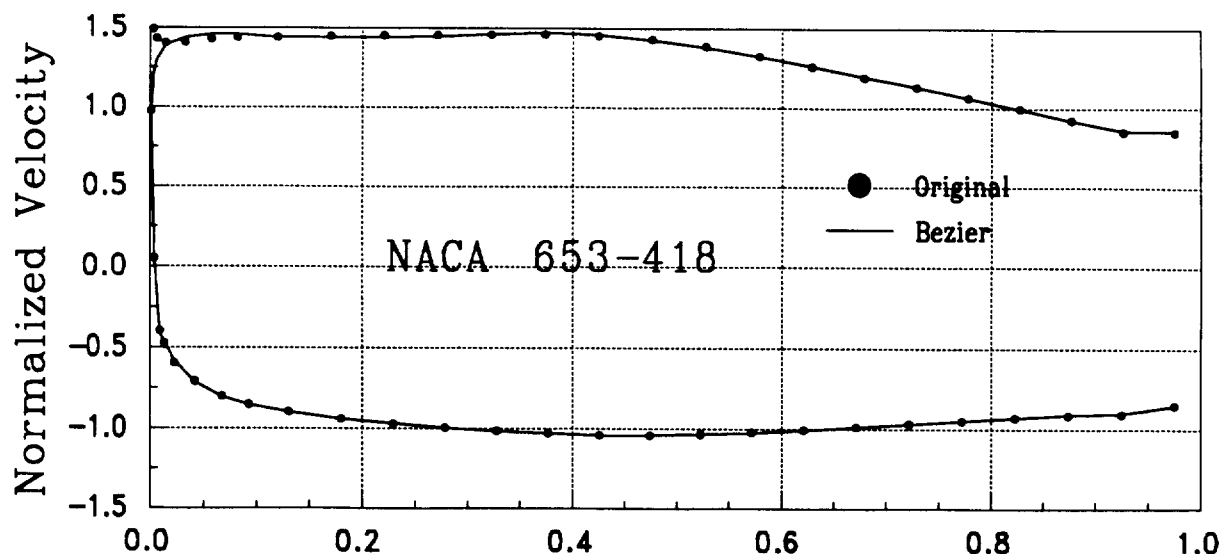


Figure 5. NACA 653-418 - Velocity Distribution

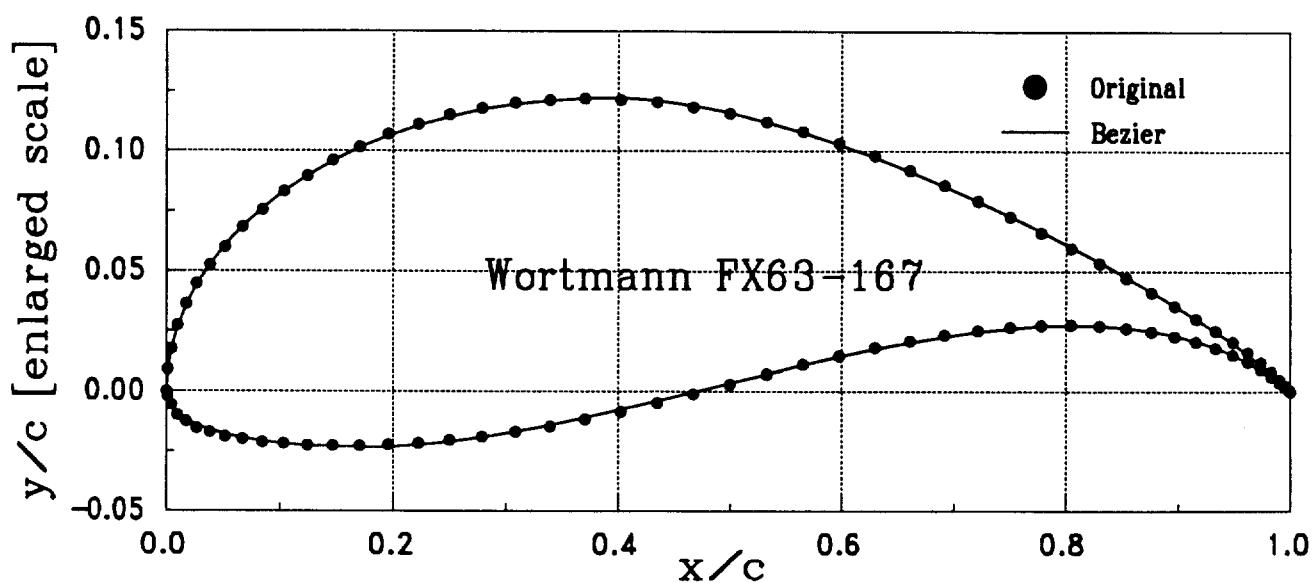


Figure 6. Wortmann FX63-167 - Original and Bezier

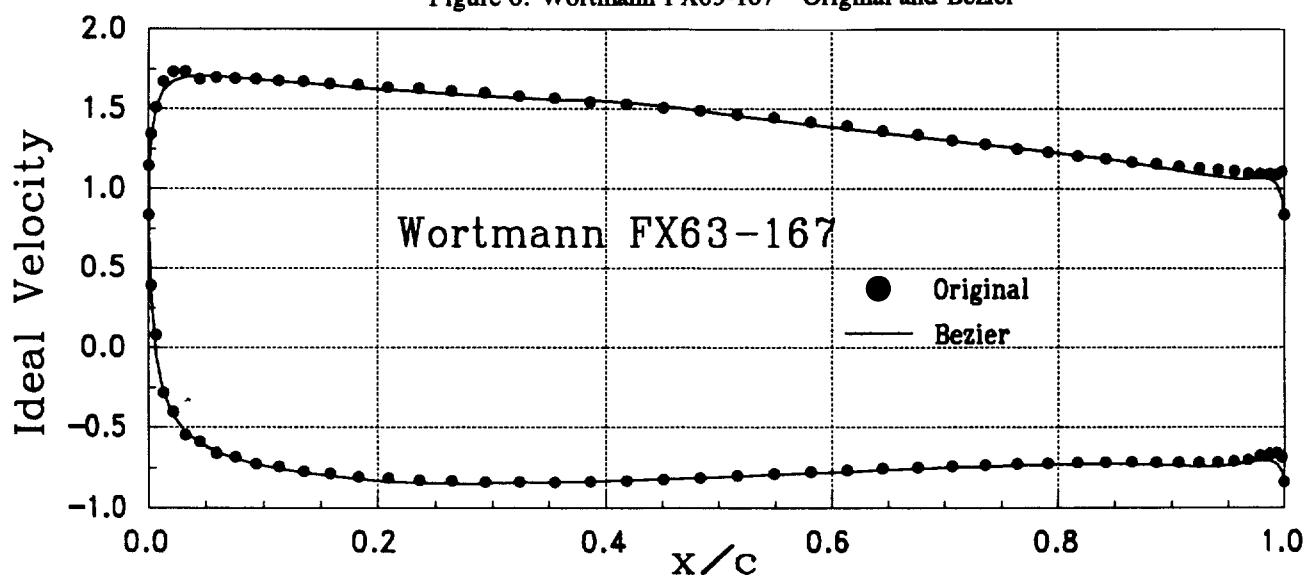


Figure 7. Wortmann FX63-167 Velocity Distribution



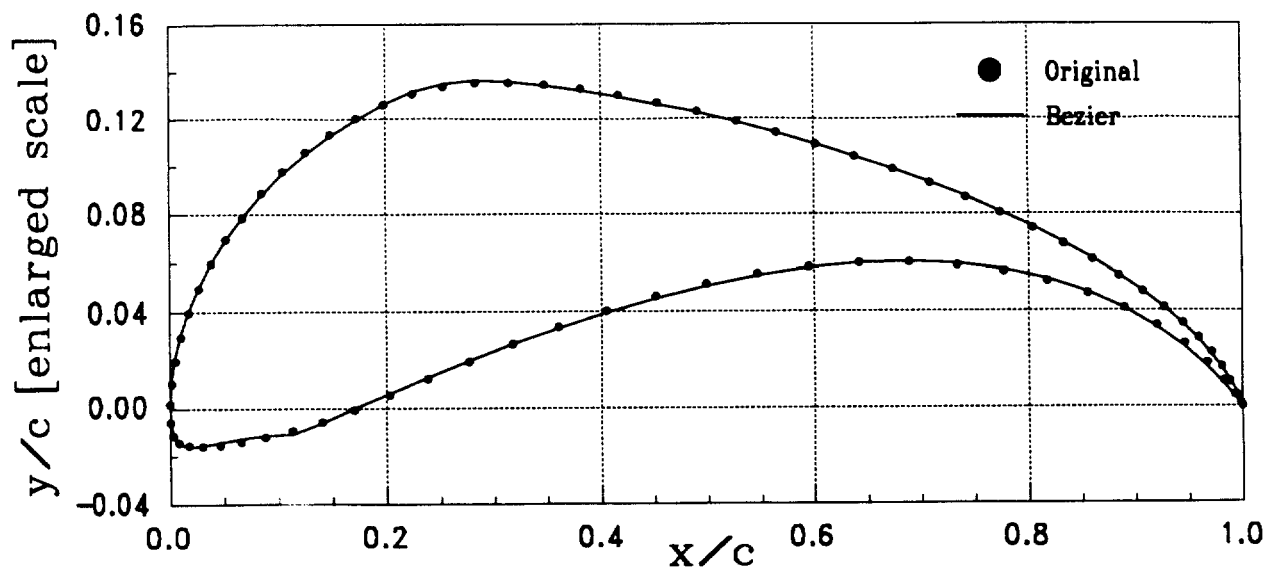


Figure 8. Selig S1223 - Original and Bezier

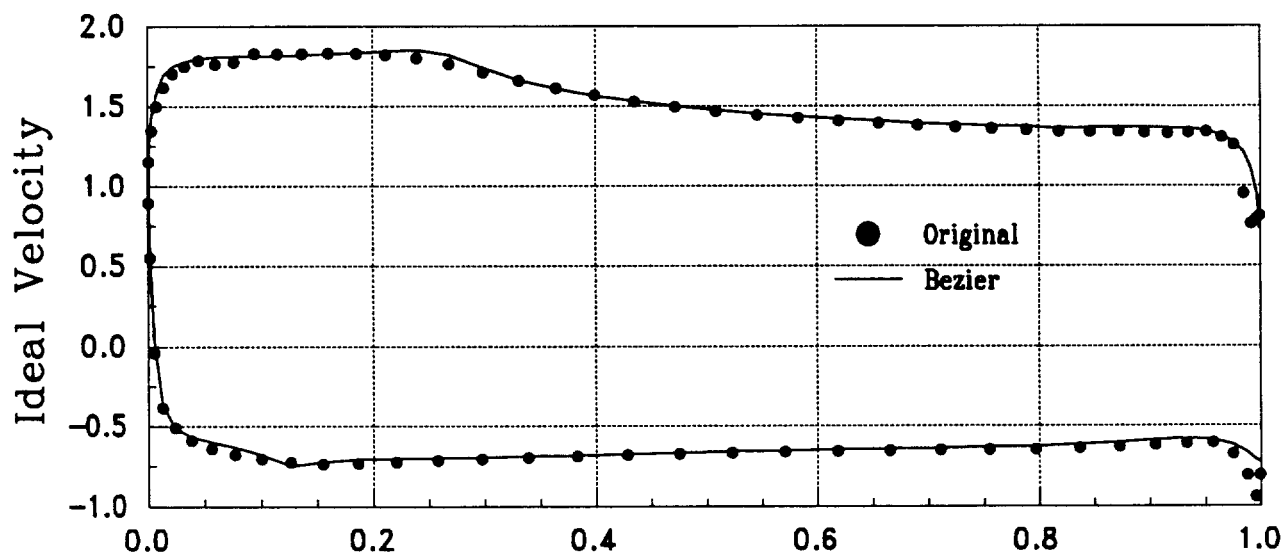


Figure 9. Selig S1223 - Velocity Distribution

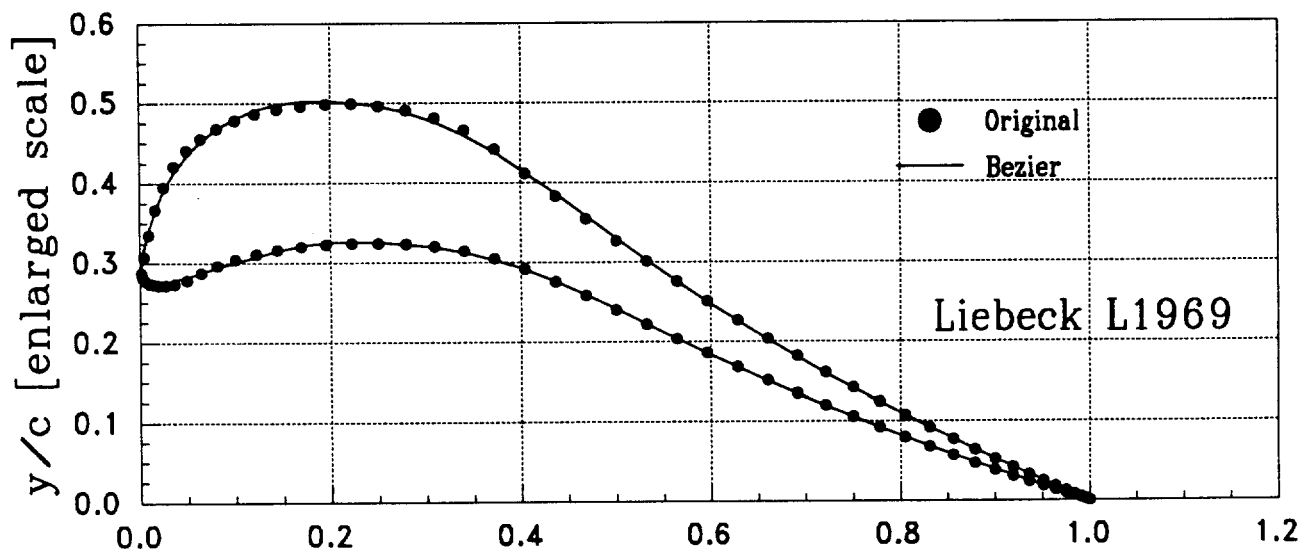


Figure 10. Liebeck L1969 - Original and Bezier

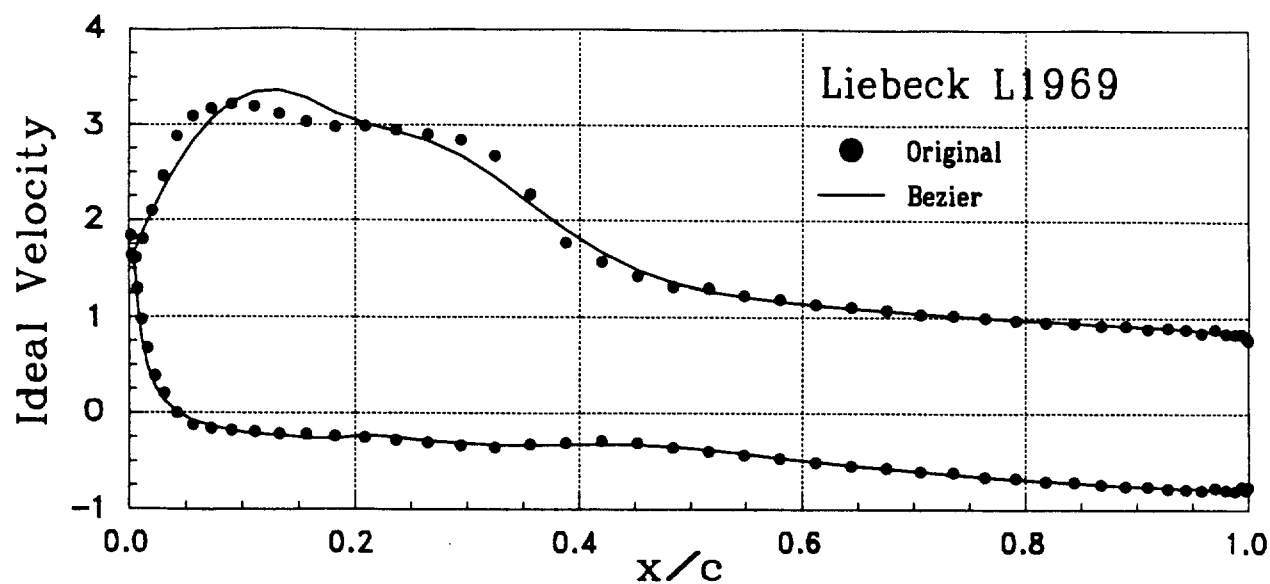


Figure 11. Liebeck L1969 - Velocity Distribution

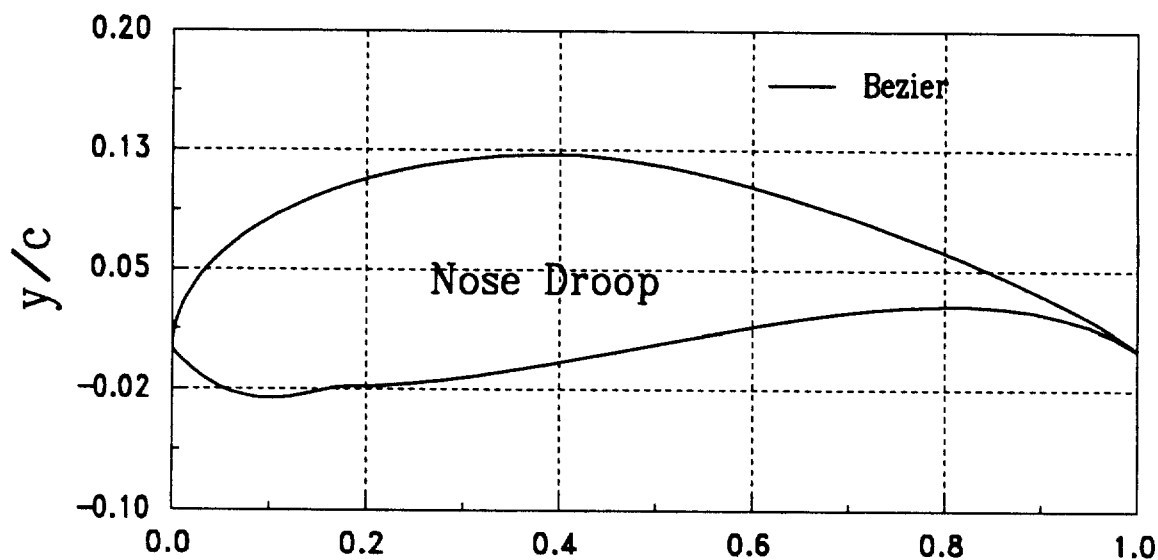


Figure 12. Example of Droop Nose

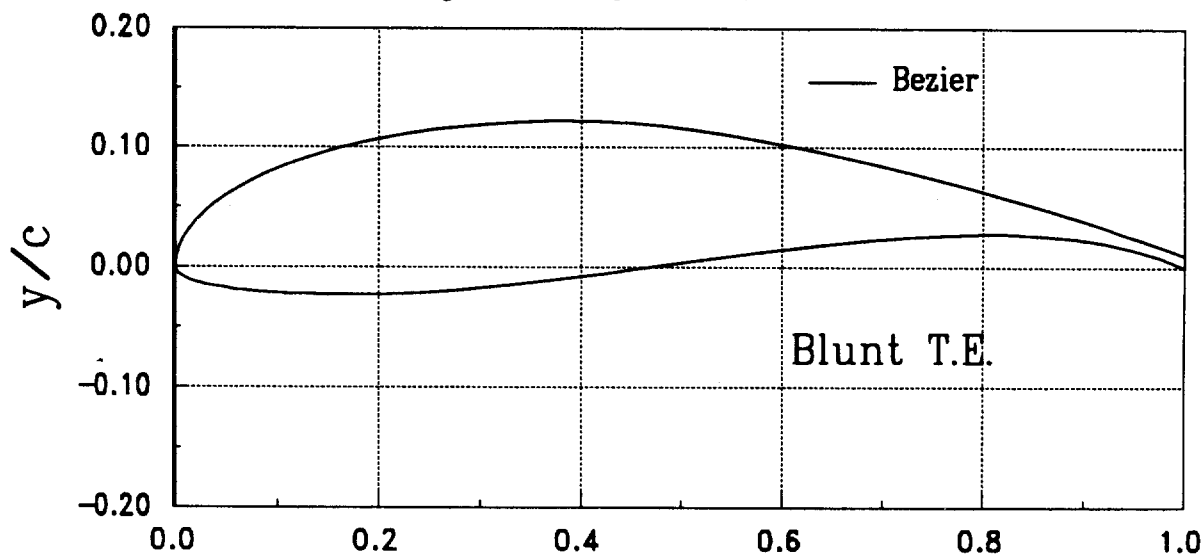


Figure 13. Example of a Blunt Trailing Edge